

THE RELATIVE MOTION OF EARTH ORBITING SATELLITES

EDWIN WNUK and JUSTYNA GOLEBIEWSKA

*A. Mickiewicz University, Astronomical Observatory, Słoneczna 36, PL 60-286 Poznan, Poland,
e-mail: wnuk@amu.edu.pl; jg@amu.edu.pl*

(Received: 4 November 2003; revised: 20 September 2004; accepted: 4 October 2004)

Abstract. Relative motion of objects moving in a close satellite formation is studied. The relative motion is expressed in the satellite reference frame RAB defined by orthogonal unit vectors in the radial, transverse and normal directions. Differential perturbations in orbital elements, satellite positions as well as in the radial, transverse and normal components of the radius vector are defined. Differential perturbations due to geopotential coefficients and lunisolar attraction are analysed for some exemplary satellites orbits. Results of a numerical analysis of motion have shown that the geopotential coefficients up to high degree and order as well as lunisolar effects have to be included into the applied force model to save the meter or centimeter level of accuracy in the description of the relative satellite motion.

Key words: differential perturbations, formation flying

1. Introduction

It is planned that many future space missions will utilize satellite constellations or formation flying. Satellite formation is a cluster of distributed small cooperative units performing the function of a single complex satellite. These clusters of satellites usually work together and fly in a precise formation. Increased productivity and reduced mission launch costs are important benefits of the use of satellite formation as opposed to single large spacecraft.

One of the first formations was the Landsat7-Earth Observing-1. On the 17 of May 2001 the Earth Observing-1 was inserted into a 705 km circular, sun-synchronous orbit at a 98.7° inclination, so that it was flying in formation 1 min behind Landsat 7 in the same ground track. Similar formation is made by two satellites realizing the Gravity Recovery and Climate Experiment (GRACE) mission.

Satellite constellations and formation flying is planned to be used in a number of varied scientific, military, and satellite service operations. For example the Darwin and Terrestrial Planet Finder (TPF) missions will be realized as satellite formations consisting of a number of components.

Another example of a mission that will use formation flying (to study atmospheric phenomena) is the Leonardo-BRDF mission. For Leonardo the

satellite formation includes one chief (on the orbit $I = 5^\circ$, $e = 0$, $h = 400$ km) and six deputy microsattellites.

To meet the mission goals, the shape of the formation and relative distances between the formation units have to be preserved to an appropriate accuracy. For some missions (e.g., space interferometry) the accuracy requirements are very high (centimeters or even millimeters). On the other hand, in geodetic missions like GRACE the satellite-to-satellite (SST) range and range-rate data are used to improve the Earth gravity field with high resolution. These data measure the difference between the position perturbations of two satellites to a very high accuracy (on a micrometer level). To fully exploit the geopotential information contained in the range and range-rate data, an accurate theory is necessary for understanding the nature of the gravitational perturbation spectrum for the SST measurements (Cheng, 2002). Dynamical aspects of formation flying are then a crucial issue.

Dynamics of spacecrafts flying in a precise formation was a subject of numerous papers in the last few years. In most cases, the authors of these papers have used the classical Hill equations for description of the relative motion of the deputy and chief satellites. These equations assume that the Earth is spherically symmetric and the chief reference orbit is circular. In more precise descriptions of a relative satellite motion the effect of eccentric spacecraft trajectories and the influence of J_2 are considered as the main perturbation factors (Alfriend et al., 2000; Gim and Alfriend, 2000, 2005). Thus, the perturbation force model in the relative motion is commonly restricted to the second zonal harmonic J_2 .

However, the neglected disturbing forces, may produce significant perturbation effects. Sabol et al., (2001) analyzed the influence of different perturbation factors on the stability of four types of satellite formation designs. They took into account circular or near circular orbits of the same values of the mean semi-major axis of all satellites in a given formation. Starting from the mean orbital elements and using the Draper Semianalytic Satellite Theory (Neelson et al., 1998) the authors propagated the mean orbital elements of the formation's units over a given time span. A distance between satellites was relatively stable only in the in-plane and in-track formations. For the out-of-plane formations significant secular changes in the separation between the formation units were observed.

For large aperture formations (e.g., circular formations) some satellites perform out-of-plane motion relative to the reference orbit. This out-of-plane motion is achieved by some combination of changes in the inclination and the longitude of ascending node. Differences in these orbital elements result in different values of secular perturbations and different amplitudes of periodic and resonance perturbations. Precise description of the relative motion of satellites orbiting in a cluster should take into regard, besides J_2 , also the

influence of other geopotential harmonic coefficients, atmospheric drag, solar radiation pressure and luni-solar effects.

Analytical perturbation theory for intersatellite range and range-rate measurements between two satellites has been recently published by Cheng (2002). This theory includes perturbations due to geopotential and the Earth tides and takes into account only the in-plane motion. Here, we study the relative satellite motion without any restriction as to the plane of the satellite orbits as well as their eccentricity and inclination. In our analysis we take into account the influence of geopotential and luni-solar perturbations.

The numerical results presented in this paper were obtained by numerical integration of the equations of motions of individual members of a formation. As opposed to Sabol et al., (2001) we used osculating orbital elements to calculate the starting values of the satellite positions and velocities. The osculating elements are more useful in practice than the mean elements. On the one hand, they are determined directly from observations of satellite positions and they are used in calculations of relative positions of the formation units in the space.

An application of the mean elements in a description of the relative motion in a formation needs very precise algorithm of the transformation between the osculating and the mean elements. The transformation as well as an analytical theory of relative satellite motion that takes into account all important perturbations will be a subject of separate papers.

2. Differential Perturbations

We consider the relative motion of two satellites S_1 and S_2 . Let $\varepsilon_n^1(t)$ and $\varepsilon_n^2(t)$, $n = 1, 2, \dots, 6$ represent six osculating orbital elements of S_1 and S_2 , respectively at the time moment t . Then $\Delta\varepsilon_n(t) = \varepsilon_n^2(t) - \varepsilon_n^1(t)$, $i = 1, 2$, are differences between the osculating orbital elements of these two satellites. The positions and velocities in the geocentric reference frame corresponding to the elements $\varepsilon_n^i(t)$ are represented by $\vec{r}^i(t)$ and $\dot{\vec{r}}^i(t)$. The separation between two satellites is then given by

$$\Delta\vec{r}(t) = \vec{r}^2(t) - \vec{r}^1(t). \quad (1)$$

Let now $\varepsilon_{0,n}^i$, $i = 1, 2$, $n = 1, 2, \dots, 6$ represent six orbital elements of the unperturbed orbits of satellites S_1 and S_2 and $\vec{r}_0^i(t)$ and $\dot{\vec{r}}_0^i(t)$ are positions and velocities of S_1 and S_2 on the unperturbed orbits at the moment t . Then

$$\delta\varepsilon_n^i(t) = \varepsilon_n^i(t) - \varepsilon_{0,n}^i(t) \quad (2)$$

are perturbations in the orbital elements, and

$$\delta\vec{r}^i(t) = \vec{r}^i(t) - \vec{r}_0^i(t) \quad (3)$$

are perturbations in the satellite positions. Differences

$$\Delta(\delta\epsilon(t)) = \delta\epsilon_n^1(t) - \delta\epsilon_n^2(t) \quad (4)$$

and

$$\Delta(\delta\vec{r}(t)) = \delta\vec{r}^1(t) - \delta\vec{r}^2(t) \quad (5)$$

are the differential perturbations in the orbital elements and in the satellite positions, respectively.

3. Perturbations in Radial, Transverse and Normal Components

The relative motion of two satellites S_1 and S_2 may be expressed in the satellite orbital reference frame $R\Lambda B$ (Figure 1) defined by orthogonal unit vectors in the radial r , transverse (along-track) λ and normal (cross-track) b directions. Denote the unit vectors in these three directions for the i th satellite as \vec{e}_1^i (radial), \vec{e}_2^i (transversal) and \vec{e}_3^i (normal), $i = 1, 2$. The unit vectors \vec{e}_k^i can be expressed in terms of the orbital elements: inclination I , ascending node Ω and the argument of latitude $u = \omega + f$ (Taff, 1985):

$$\begin{aligned} \vec{e}_1^i &= [\cos\Omega\cos u - \sin\Omega\sin u\cos I, \sin\Omega\cos u + \cos\Omega\sin u\cos I, \sin u\sin I]^T, \\ \vec{e}_2^i &= [-\cos\Omega\sin u - \sin\Omega\cos u\cos I, -\sin\Omega\sin u + \cos\Omega\cos u\cos I, \cos u\sin I]^T, \\ \vec{e}_3^i &= [\sin\Omega\sin I, -\cos\Omega\sin I, \cos I]^T. \end{aligned} \quad (6)$$

Denote the direction cosines of the unit vectors for the i th satellite in the $R\Lambda B$ frame of the j th satellite as α_{ij}

$$\alpha_{ij} = \vec{e}_i^1 \cdot \vec{e}_j^2. \quad (7)$$

In general, the direction cosines are functions of orbital elements of both satellites and can be expressed in terms of $dI = I^2 - I^1$, $d\Omega = \Omega^2 - \Omega^1$ and/or $du = u^2 - u^1$. Formula for α_{ij} for arbitrary values of dI , $d\Omega$ and du are given in

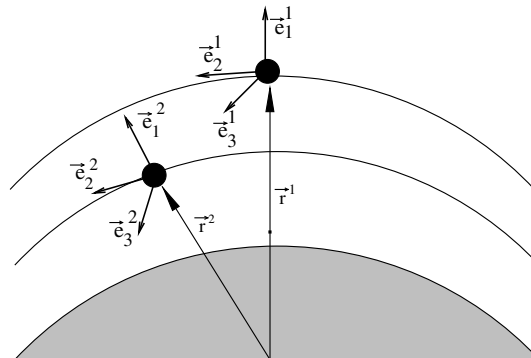


Figure 1. Unit vectors in the $R\Lambda B$ frame.

Appendix A.1. For coplanar orbits of S_1 and S_2 , when $dI = 0$, $d\Omega = 0$ and du is of an arbitrary value, the formulas for α_{ij} are given in Appendix A.2.

And finally, when the satellites move, in general, on orbits with different values of the inclination I and the ascending node Ω , but the differences dI , $d\Omega$ and du are small enough to meet the following conditions:

$$\begin{aligned} \sin di &= di, & \sin d\Omega &= d\Omega, & \sin du &= du, \\ \cos di &= 1, & \cos d\Omega &= 1, & \cos du &= 1. \end{aligned} \quad (8)$$

with the accuracy ε that is sufficient in calculations, the formulas for the direction cosines are very simple (see Appendix A.3). The above conditions mean that we consider the satellite formation with individual units moving on slightly different orbits and/or slightly different positions on the same orbit. The last formulas for the direction cosines are very useful in an analytical description of the relative satellite motion, particularly when the direction cosine matrix is applied in a transformation of perturbations from the reference frame of the satellite S_1 to the reference frame of satellite S_2 (see Equation (13)). In this case the accuracy $\varepsilon = 10^{-6}$ is sufficient. The results of the calculations presented in the next paragraph were obtained by numerical integration with the use of the general form of the direction cosines (Appendix A.1). Note however, that for the orbits of satellites used in these calculations, when the differences of the angular orbital elements of two satellites in a given pair are 0.05° , the conditions (8) are kept with the accuracy ε better than 10^{-6} . In this case the approximated formulas for direction cosines given in Appendix A.3 introduce an error on a level lower than 10^{-9} in Equation (13), which may be neglected in the calculations.

The satellite positions and perturbations in the satellite position in the orbital reference frame RAB may be expressed in the following form:

$$\vec{r}^i = r^i \vec{e}_1^i, \quad (9)$$

$$\delta \vec{r}^i = \delta r^i \vec{e}_1^i + \delta \lambda^i \vec{e}_2^i + \delta b^i \vec{e}_3^i, \quad (10)$$

where $r^i = |\vec{r}^i|$, and δr^i , $\delta \lambda^i$, δb^i are the radial, transverse and normal components of the perturbations in the i th satellite position.

The analytical formulas for perturbations in the radial, transverse and normal components as functions of the true anomaly f have the following form (e.g., Casotto, 1993):

$$\begin{aligned} \delta r &= \frac{r}{a} \delta a - a \delta e \cos f + \frac{ae}{\sqrt{1-e^2}} \delta M \sin f, \\ \delta \lambda &= r(\delta \Omega \cos I + \delta \omega) + \frac{a}{r} a \sqrt{1-e^2} \delta M + a \delta e \left(\frac{1}{1-e^2} \frac{r}{a} + 1 \right) \sin f, \\ \delta b &= r(\delta I \sin(f + \omega)) - \delta \Omega \sin I \cos(f + \omega). \end{aligned} \quad (11)$$

where δa , δe , δM , $\delta \Omega$, $\delta \omega$, δI are perturbations in the Keplerian elements.

Differential perturbations in satellite positions can be expressed in terms of the reference frame RAB of the satellite S_1 in the following form:

$$\Delta(\delta\vec{r}(t)) = \delta\vec{r}^1 - \delta\vec{r}^2 = \Delta r^1 \vec{e}_1^1 + \Delta\lambda_1 \vec{e}_2^1 + \Delta b_1 \vec{e}_3^1, \quad (12)$$

where

$$\begin{aligned} \Delta r^1 &= \delta r^1 - \delta r^2 \alpha_{11} - \delta\lambda^2 \alpha_{12} - \delta b^2 \alpha_{13}, \\ \Delta\lambda^1 &= \delta\lambda^1 - \delta r^2 \alpha_{21} - \delta\lambda^2 \alpha_{22} - \delta b^2 \alpha_{23}, \\ \Delta b^1 &= \delta b^1 - \delta r^2 \alpha_{31} - \delta\lambda^2 \alpha_{32} - \delta b^2 \alpha_{33}, \end{aligned} \quad (13)$$

where $\Delta r, \Delta\lambda$ and Δb are differential perturbations in the radial, transverse and normal components of the radius vector.

Here, for the calculations of the differential perturbations components, we applied the following relations:

$$\begin{aligned} \delta r &= \delta x \vec{i}_x \cdot \vec{e}_1 + \delta y \vec{i}_y \cdot \vec{e}_1 + \delta z \vec{i}_z \cdot \vec{e}_1, \\ \delta\lambda &= \delta x \vec{i}_x \cdot \vec{e}_2 + \delta y \vec{i}_y \cdot \vec{e}_2 + \delta z \vec{i}_z \cdot \vec{e}_2, \\ \delta b &= \delta x \vec{i}_x \cdot \vec{e}_3 + \delta y \vec{i}_y \cdot \vec{e}_3 + \delta z \vec{i}_z \cdot \vec{e}_3, \end{aligned} \quad (14)$$

where $\vec{i}_x, \vec{i}_y, \vec{i}_z$ are the unit versors of the $Oxyz$ reference frame, $\vec{e}_1, \vec{e}_2, \vec{e}_3$ are given by Equation(6), and $\delta x, \delta y, \delta z$ are perturbations in the x, y, z coordinates obtained from Equation (3) with the use of numerical integration of equations of motion of the satellites S_1 and S_2 . Then applying Equation (13), we calculated the differential perturbations in the radial, transverse and normal components.

4. Influence of Geopotential and Luni-Solar Perturbations on the Relative Motion of Satellites

When separation requirements among members of a formation are hundreds of meters or kilometers, it is sufficient to include in the perturbation model only the main perturbation factors. Usually, in these cases the perturbation model is restricted to the second zonal harmonic coefficient J_2 only. However, when relative positions between satellites have to be maintained to a very high accuracy level (meters or centimeters), other forces acting on the satellites cannot be neglected.

A few examples given below illustrate the influence of geopotential and luni-solar perturbations on the relative orbits of two satellites. The orbital elements of the satellites used in the exemplary calculations are given in Table I. The orbits of the first pair of the satellites are similar to the Leonardo-BFDF formation orbits of the altitude 400 km and 5° inclination. The second pair of satellites move on the 1400 km altitude orbits with the eccentricity equal 0.05 and the inclination of 85° .

TABLE I
Orbital elements of satellites.

Pair	Satellite	a (km)	e	I (°)	ω (°)	Ω (°)	M (°)	Initial separation (m)
I	1	6778	0.001	5.00	60	0.00	0.0	7640
I	2	6778	0.001	5.05	60	0.05	0.0	7640
II	1	7800	0.05	85.00	60	0.00	0.0	2444
II	2	7800	0.05	85.05	60	0.05	0.0	2444

In order to estimate the influence of a given disturbing factor on differential perturbations in orbits of two satellites S_1 and S_2 we calculated these perturbations with the use of two perturbation models: mod1 and mod2 that differ from each other by the disturbing factor considered. The differential perturbations in positions of both satellites (Equation (5)) were obtained by numerical integration of the equations of motion in rectangular coordinates. The initial values of position and velocities at the time t_0 were calculated from the orbital elements given in Table I. Starting with the same initial conditions for the perturbation models mod1 and mod2, we integrated the orbits of satellites S_1 and S_2 and calculated the differential perturbations for both models. Next, by comparison of these differential perturbations $\Delta(\delta\vec{r}(t))_{\text{model1}} - \Delta(\delta\vec{r}(t))_{\text{model2}}$ we estimated the influence of the perturbation factor on the value of the differential perturbation. First, we estimated the influence of the second zonal harmonic on the relative positions of satellites S_1 and S_2 . We integrated numerically the motion of these satellites over 10 day time span with the use of the following two force models: (1) Keplerian – without any perturbation effects and (2) J_2 -model – the influence of the second zonal harmonic was included. Results are presented in Figures 2 and 3. For pair I the differences in the differential perturbations after 10 days are of the order of 14 km, and for pair II these differences are of the order of 20 km. Secular and periodic effects are observed for both pairs. Figures 4 and 5 present differences in the differential perturbations for pairs I and II, respectively, obtained within the following two force models: (1) J_2 -model and (2) 15×15 model including all zonal and tesseral harmonic coefficients up to degree and order 15. Therefore, these differences represent the differential perturbation effect due to the zonal harmonics $J_n, 2 < n < 15$ and the tesseral harmonics up to order and degree 15. After 10 day time span the differences are on the level of 150 m and 40 m for the pairs I and II, respectively. Again, secular and periodic effects are observed for both pairs of satellites.

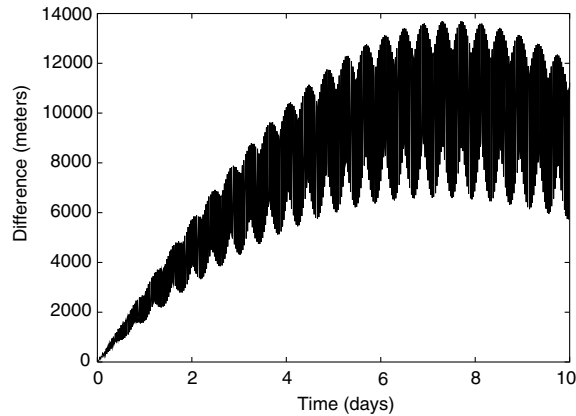


Figure 2. Differences in differential perturbations for pair I of satellites calculated with the use of following force models: (1) unperturbed Keplerian and (2) J_2 -model.

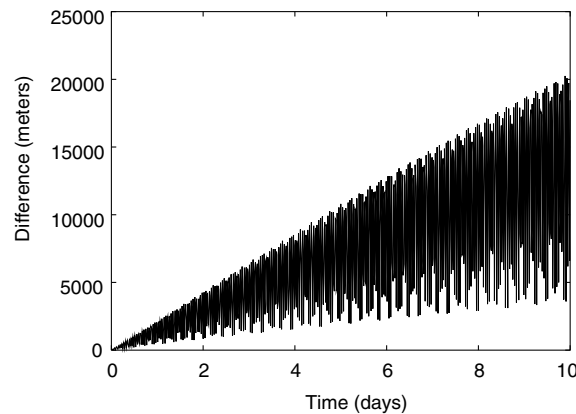


Figure 3. Differences in differential perturbations for pair II of satellites calculated with the use of the following forcer models: (1) unperturbed Keplerian and (2) J_2 model.

Note, however, that the differences in the differential perturbations strongly depend on the initial conditions. Figure 6 shows the differences in the differential perturbations for pair I for the two following cases: (1) the mean anomaly M was changed from 0° to 60° and (2) the mean anomaly M was changed from 0° to 80° . Comparing the results from Figure 6 with those from Figure 4 (where $M = 0^\circ$) one may observe significant differences. Therefore, the numerical analysis presented in this paper only indicates an order of the perturbations effects. For a specific formation mission orbits one has to make detailed analysis of perturbation effects taking into account the real initial conditions.

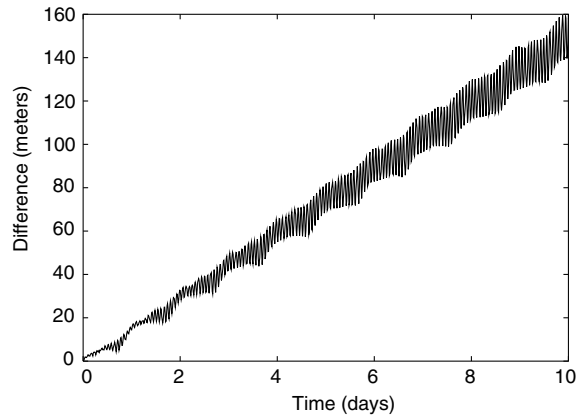


Figure 4. Differences in differential perturbations for pair I of satellites calculated with the use of following force models: (1) J_2 -model and (2) 15×15 model.

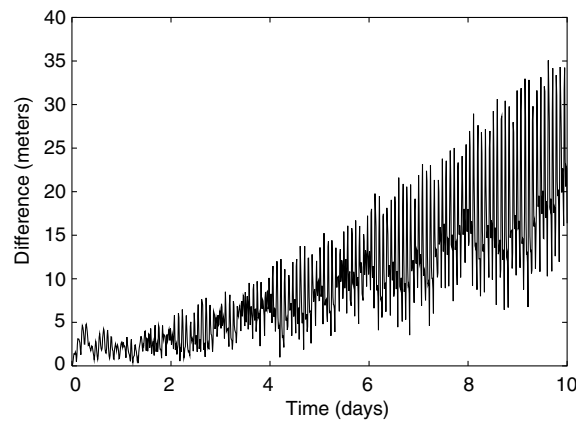


Figure 5. Differences in differential perturbations for pair II of satellites calculated with the use of following force models: (1) J_2 -model and (2) 15×15 model.

In the second step of the numerical analysis of the differential geopotential perturbations we tried to answer the following question: what is the maximum order and degree of geopotential harmonic coefficients that have to be included into the force model to save a given accuracy level. To this end we calculated numerically the differential perturbations taking into account all geopotential coefficients C_{lm} and S_{lm} with a given order m and all possible (in the applied geopotential model) degrees l . The values of differential perturbation for pairs I and II are shown in Figures 7 and 8, respectively. For pair I the differential perturbation effects are on a level of 100 m for harmonic orders up to 6 and all coefficients up to at least order

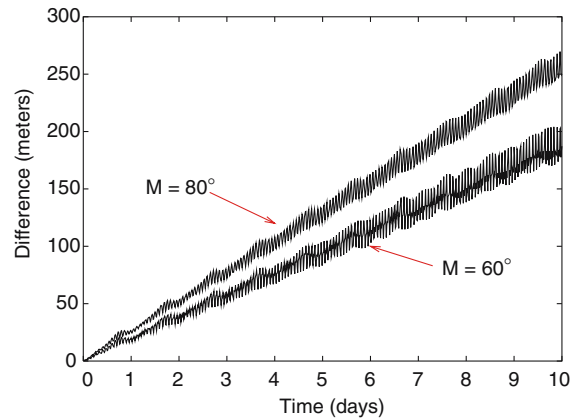


Figure 6. Differences in differential perturbations for the pair I of satellites with initial value of the mean anomaly M changed to 60° and 80° .

70 have to be taken into account to save the 10 cm accuracy in the determination of the relative satellite positions in this case. For higher orbits of satellites in pair II (1400 km altitude) it is sufficient to include geopotential coefficients up to the order 40 to save the 1 cm accuracy (Figure 8).

Next, the total values of differential perturbations due to individual harmonic orders presented in Figures 7 and 8 were decomposed into the radial, transverse and normal components with the use of Equations (13) and (15). Figures 9 and 10 present values of the components of the differential perturbations for satellites in pairs I and II, respectively. For both pairs the transverse components of the differential perturbations are much higher than the radial and normal components.

Finally, we estimated values of differential perturbations due to lunisolar effects. Tables II–IV presents values of lunar, solar and combined luni-solar differential perturbations obtained by numerical integration of satellite motion on a 10 day time span. For low altitude orbits of pair I these perturbations are on a level of 2 m. For pair II the differential perturbations due to luni-solar effects are higher and can reach 3.5 m. Note, that the values of the luni-solar differential perturbations increase with the increasing semi-major axis of satellites moving in a formation. The maximum value of total luni-solar differential perturbations over 10 days time span for satellites at the 20000 km and 36000 km altitude is on the level of 40 and 150 m respectively.

The results presented in this paragraph were obtained by numerical integration of equations of perturbed satellite motion with the use of initial conditions (positions and velocities at the time t_0) calculated directly

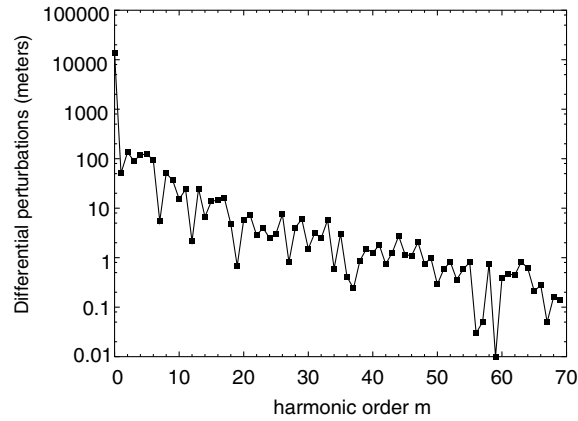


Figure 7. Maximum values of differential perturbations in the motion of the satellites from the pair I due to geopotential spherical coefficients C_{lm}, S_{lm} of the individual orders m calculated over 10 day span.

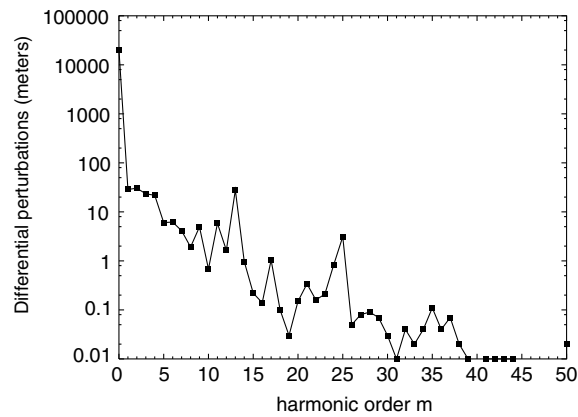


Figure 8. Maximum values of differential perturbations in the motion of the satellites from the pair II due to geopotential spherical coefficients C_{lm}, S_{lm} of the individual orders m calculated over 10 day span.

from orbital elements given in Table I. This means that we treated the initial orbital elements as osculating. In each pair, the satellites S_1 and S_2 have the same values of the osculating semi-major axis and eccentricity. However, the mean values of semi-major axis and the values of the mean motion as well as the mean values of other elements of both satellites in a given pair may differ. Therefore, the differential perturbations obtained by numerical integration depend not only on perturbing forces acting on the satellites, but also on the choice of the initial orbital elements. To reduce the growth of magnitude of a separation between satellites due to the

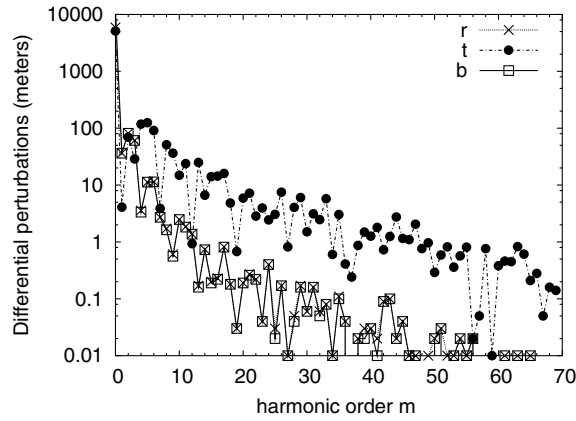


Figure 9. Maximum values of the radial, transverse and normal components of differential perturbations in the motion of pair I satellites due to geopotential spherical coefficients C_{lm}, S_{lm} of the individual orders m calculated over 10 day span.

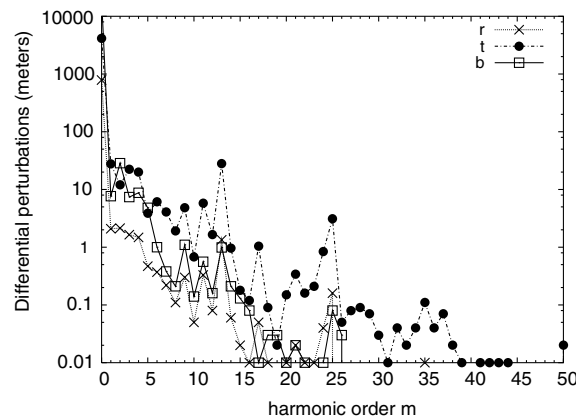


Figure 10. Maximum values of the radial, transverse and normal components of differential perturbations in the motion of pair II satellites due to geopotential coefficients C_{lm}, S_{lm} of the individual orders m calculated over 10 day span.

differential perturbations one has to choose the initial osculating elements of satellites in a given formation in such a way that the corresponding mean elements have the same values of the semi-major axis of all satellites in the formation. To this end a transformation between the osculating and mean orbital elements on an appropriate high accuracy level is needed. Sabol et al. (2001) used the mean orbital elements and the semi-analytical theory in their analysis of the influence of different perturbing factors on the stability of the separation between satellites in some types of

TABLE II
Maximum values of differential lunar perturbations in meters over a 10 day span.

Satellite pair	Total perturbations	Radial perturbations	Transverse perturbations	Normal perturbations
I	1.73	0.52	1.64	0.34
II	2.11	0.30	2.07	0.39

TABLE III
Maximum values of differential solar perturbations in meters over a 10 day span.

Satellite pair	Total perturbations	Radial perturbations	Transverse perturbations	Normal perturbations
I	0.59	0.11	0.57	0.19
II	1.52	0.21	1.52	0.28

TABLE IV
Maximum values of differential luni-solar perturbations in meters over a 10 day span.

Satellite pair	Total perturbations	Radial perturbations	Transverse perturbations	Normal perturbations
I	2.28	0.63	2.21	0.30
II	3.61	0.50	3.59	0.36

formations. We recalculated the examples presented by Sabol et al. using our method presented above and we obtained comparable results. The initial osculating elements used in these calculations were obtained from the mean orbital elements given by Sabol et al. with the use of the transformation from mean to osculating elements based on the second order analytical theory of perturbations (Wnuk, 1995).

5. Conclusion

The results of the numerical analysis of differential perturbations in the orbits of satellites moving in a close formation presented in this paper were obtained by numerical integration. The analysis has been made taking into account only the luni-solar and geopotential perturbations due to arbitrary degree and order of spherical harmonics. The results show that for the precise (on meter or centimeter accuracy level) description of a relative satellite

motion one has to take into account a force model that includes other effects besides the second zonal harmonic J_2 . For very low altitude orbits and for the case when the relative positions of formation members have to be known with the meter or centimeter accuracy, the force model should include the influence of all zonal and tesseral harmonic coefficients of a geopotential model up to 70 degree and order. The values of the luni-solar differential perturbations are small (about 2–3 m or less after 10 days), but they increase with increasing semi-major axis of the satellites orbits. Note, that the perturbations effects due to atmospheric drag and solar radiation pressure neglected in this paper for some formations may produce differential perturbations on a level comparable with luni-solar and higher degree and order geopotential harmonic effects.

The numerical results presented in this paper show only an order of differential perturbation effects. For given satellite formation orbits more detailed analysis has to be done.

The force model adopted in the calculations of the differential perturbations depends on the formation accuracy requirements. For example, for geodetic formations like GRACE, when very precise (on a level of millimeters) relative range and range-rate measurements are analyzed, the description of the relative satellite motion has to include differential perturbations with all possible effects (with high order and degree geopotential harmonics included). On the other hand, in the case of formations when the accuracy requirements concerning the relative positions of individual units are lower e.g., on a meter level, the model of the differential perturbations may be restricted in the appropriate way including, for example only a few important geopotential harmonics.

The differential perturbations strongly depend on the initial orbital elements of all satellites moving in a formation. The proper choice of the initial osculating orbital elements of the individual formation units may significantly reduce the magnitude of differential perturbations. This choice may be done only on the basis of the analytical transformation between the osculating and mean orbital elements that includes all perturbations taken to the appropriate accuracy.

Acknowledgements

This work was supported by the State Committee for Scientific Research (KBN) under the grant No 8T12E 02820.

Appendix A. The Direction Cosines

A.1. Direction cosines α_{ij} for arbitrary values of δI , $\delta\Omega$ and δu .

$$\begin{aligned}\alpha_{11} &= \vec{e}_1^1 \cdot \vec{e}_1^2 = (1/2 \sin 2I_1 \sin dI + \cos dI \sin^2 I_1) \sin u_1 \sin u_2 \\ &\quad + \sin d\Omega (\cos I_1 \cos u_2 \sin u_1 - \cos(dI + I_2) \cos u_1 \sin u_2) \\ &\quad + \cos d\Omega (\cos u_1 \cos u_2 + \cos dI \cos^2 I_1 \sin u_1 \sin u_2 \\ &\quad \quad - 1/2 \sin 2I_1 \sin dI \sin u_1 \sin u_2), \\ \alpha_{12} &= \vec{e}_1^1 \cdot \vec{e}_2^2 = (1/2 \sin 2I_1 \sin dI + \cos dI \sin^2 I_1) \sin u_1 \cos u_2 \\ &\quad - \sin d\Omega (\cos(dI + I_1) \cos u_1 \cos u_2 + \cos I_1 \sin u_1 \sin u_2) \\ &\quad + \cos d\Omega (\cos dI \cos^2 I_1 \sin u_1 \cos u_2 \\ &\quad \quad - 1/2 \sin dI \sin 2I_1 \sin u_1 \cos u_2 - \cos u_2 \sin u_2), \\ \alpha_{13} &= \vec{e}_1^1 \cdot \vec{e}_3^2 = \sin d\Omega \cos u_1 \sin(dI + I_1) + 1/2 \cos dI \sin 2I_1 \sin u_1 \\ &\quad - \cos d\Omega \sin u_1 (\sin dI \cos^2 I_1 + 1/2 \cos dI \sin 2I_1) \\ &\quad - \sin dI \sin^2 I_1 \sin u_1, \\ \alpha_{21} &= \vec{e}_2^1 \cdot \vec{e}_1^2 = (1/2 \sin 2I_1 \sin dI + \cos dI \sin^2 I_1) \cos u_1 \sin u_2 \\ &\quad + \sin d\Omega (\cos I_1 \cos u_1 \cos u_2 + \cos(dI + I_1) \sin u_1 \sin u_2) \\ &\quad + \cos d\Omega (\cos dI \cos^2 I_1 \cos u_1 \sin u_2 \\ &\quad \quad - 1/2 \sin 2I_1 dI \cos u_1 \sin u_2 - \sin u_1 \cos u_2), \\ \alpha_{22} &= \vec{e}_2^1 \cdot \vec{e}_2^2 = (1/2 \sin 2I_1 \sin dI + \cos dI \sin^2 I_1) \cos u_1 \cos u_2 \\ &\quad + \sin d\Omega (\cos(dI + I_1) \cos u_2 \sin u_1 - \cos I_1 \cos u_1 \sin u_2) \\ &\quad + \cos d\Omega (\sin u_1 \sin u_2 + \cos dI \cos^2 I_1 \cos u_1 \sin u_2 \\ &\quad \quad - 1/2 \sin dI \sin 2I_1 \cos u_1 \cos u_2), \\ \alpha_{23} &= \vec{e}_2^1 \cdot \vec{e}_3^2 = (1/2 \cos dI \sin 2I_1 \cos u_1 \\ &\quad - \sin dI \sin^2 I_1 \cos u_1 - \sin d\Omega \sin(dI + I_1) \sin u_1 \\ &\quad - \cos d\Omega \cos u_1 (\cos^2 I_1 \sin dI + 1/2 \cos dI \sin 2I_1), \\ \alpha_{31} &= \vec{e}_3^1 \cdot \vec{e}_1^2 = -\sin d\Omega \cos u_2 \sin I_1 + \cos^2 I_1 \sin dI \sin u_2 \\ &\quad - \cos d\Omega \sin u_2 (1/2 \cos dI \sin 2I_1 - \sin dI \sin^2 I_1) \\ &\quad + 1/2 \cos dI \sin 2I_1 \sin u_2,\end{aligned}$$

$$\begin{aligned}
\alpha_{32} &= \vec{e}_3^1 \cdot \vec{e}_2^2 = \cos^2 I_1 \sin dI \cos u_2 + 1/2 \cos dI \sin 2I_1 \cos u_2 \\
&\quad - 1/2 \cos dI \sin 2I_1 \cos d\Omega \cos u_2 \\
&\quad + \sin dI \sin^2 I_1 \cos d\Omega \cos u_2 + \sin d\Omega \sin I_1 \sin u_2, \\
\alpha_{33} &= \vec{e}_3^1 \cdot \vec{e}_3^2 = \cos dI (\cos^2 I_1 + \sin^2 I_1 \cos d\Omega) \\
&\quad + 1/2 \sin dI \sin 2I_1 (\cos d\Omega - 1).
\end{aligned}$$

A.2. Direction cosines α_{ij} for coplanar orbits

$$\begin{aligned}
\alpha_{11} &= \vec{e}_1^1 \cdot \vec{e}_1^2 = \cos du, & \alpha_{12} &= \vec{e}_1^1 \cdot \vec{e}_2^2 = -\sin du, & \alpha_{13} &= \vec{e}_1^1 \cdot \vec{e}_3^2 = 0, \\
\alpha_{21} &= \vec{e}_2^1 \cdot \vec{e}_1^2 = \sin du & \alpha_{22} &= \vec{e}_2^1 \cdot \vec{e}_2^2 = \cos du & \alpha_{23} &= \vec{e}_2^1 \cdot \vec{e}_3^2 = 0, \\
\alpha_{31} &= \vec{e}_3^1 \cdot \vec{e}_1^2 = 0, & \alpha_{32} &= \vec{e}_3^1 \cdot \vec{e}_2^2 = 0, & \alpha_{33} &= \vec{e}_3^1 \cdot \vec{e}_3^2 = 1.
\end{aligned}$$

A.3. Direction cosines α_{ij} for non-zero but small values of δI , $\delta\Omega$ and δu .

$$\begin{aligned}
\alpha_{11} &= \vec{e}_1^1 \cdot \vec{e}_1^2 = 1, \\
\alpha_{12} &= \vec{e}_1^1 \cdot \vec{e}_2^2 = -du - d\Omega \cos I, \\
\alpha_{13} &= \vec{e}_1^1 \cdot \vec{e}_3^2 = d\Omega \sin I \cos u - dI \sin u, \\
\alpha_{21} &= \vec{e}_2^1 \cdot \vec{e}_1^2 = du + d\Omega \cos I, \\
\alpha_{22} &= \vec{e}_2^1 \cdot \vec{e}_2^2 = 1, \\
\alpha_{23} &= \vec{e}_2^1 \cdot \vec{e}_3^2 = -dI \cos u - d\Omega \sin I \sin u, \\
\alpha_{31} &= \vec{e}_3^1 \cdot \vec{e}_1^2 = -d\Omega \sin I \cos u + dI \sin u, \\
\alpha_{32} &= \vec{e}_3^1 \cdot \vec{e}_2^2 = dI \cos u + d\Omega \sin I \sin u, \\
\alpha_{33} &= \vec{e}_3^1 \cdot \vec{e}_3^2 = 1.
\end{aligned}$$

References

- Alfriend, K. T., Schaub, H. and Gim, D. W.: 2000, 'Gravitational perturbations, non-linearity and circular orbit assumption effects on formation flying control strategies' *Paper No., AAS 00-012, also Advances in the Astronautical Sciences* **104**, 139–158.
- Casotto, S.: 1993, 'The Mapping of Kaula's solution into the orbital reference frame', *Celest. Mech. Dyn. Astron.* **55**, 223–241.
- Cheng, M. K.: 2002, 'Gravitational perturbation theory for intersatellite tracking', *Journal of Geodesy* **76**, 169–185.

- Gim, D.-W. and Alfriend, K. T.: 2001, 'The state transition matrix of relative motion for the perturbed non-circular reference orbit', *Paper No. AAS 00-222, AAS/AIAA Space Flight Mechanics conference also. Adv. Astronaut. Sci.* **108**, 913–934.
- Gim, D.-W. and Alfriend, K. T.: 2005, 'Satellite relative motion using differential equinoctial elements', *Celestial Mechanics and Dynamical Astronomy* (in print).
- Neelson, J. G., Cefola, P. J. and Prolux, R. J.: 1998, 'Current development of the Draper Semianalytical Satellite Theory standalone orbit propagator package', AAS Paper No. 97-731, *Advances in the Astronautical Sciences* **97**, 2037–2051.
- Sabol, C., Burns, R. and McLaughlin, C. A.: 2001, 'Satellite formation flying design and evolution', *AIAA JSR* **38**(2).
- Taff, L. G.: 1985, *Celestial mechanics a Computational Guide for the Practitioner*, Wiley In., publication, New York.
- Wnuk, E.: 1995, 'Second order perturbations due to the gravity potential of a Planet', In: A. E. Roy and B. A. Steves (eds.), *From Newton to Chaos*, Plenum Press, New York, pp. 259–267.